Nanoscale deformation in TiC/a-C multilayered nanocomposite coatings

Chen, C. Q.; Pei, Y. T.; Shaha, K. P.; de Hosson, J. Th. M.

Published in:
Applied Physics Letters

DOI:
10.1063/1.2945891

Nanoscale deformation in TiC/*a*-C multilayered nanocomposite coatings

C. Q. Chen, Y. T. Pei, K. P. Shaha, and J. Th. M. De Hosson[a)]
Department of Applied Physics, The Netherlands Materials Innovation Institute, University of Groningen, Nijenborgh 4, 9747 AG Groningen, The Netherlands

(Received 16 May 2008; accepted 28 May 2008; published online 18 June 2008)

Nanoscale deformation in TiC/*a*-C nanocomposite coatings is revealed by combined nanoindentation and high resolution cross-sectional transmission electron microscopy. A process characterized by rearrangement of TiC nanocrystallites and the displacement of *a*-C matrix is found to dominate the deformation mechanism at length scales ranging from tens of nanometers down to 1 nm and contributes to toughening of the nanocomposite coatings by delocalizing local plastic deformations. © *2008 American Institute of Physics*. [DOI: 10.1063/1.2945891]

Diamondlike carbon (DLC) is an extensively studied carbon material due to its intriguing physical properties and applications.[1] DLC based nanocomposites incorporating nanosized inclusions are expected to further improve the structural and mechanical properties of pure amorphous phases.[2] However, despite the importance and extensive study on amorphous and nanocomposite carbon systems, several aspects regarding the deformation and fracture behavior at the nanoscale, and the underpinning physical mechanisms are not yet understood. Recently, several theoretical simulations have been reported on the deformation and fracture mechanism of DLC and DLC-based nanocomposite at nanometer or even subnanometer scale.[3–5] However, direct experimental validations of the theoretical models are scantly available.

Although high resolution transmission electron microscopy (HRTEM) is the most direct method to observe the effects of a mechanical response at nanometer scales, a common problem encountered in the HRTEM examination of deformed amorphous or uniformly nanostructured materials is the lack of intrinsic markers tracing microstructural changes. Recently, we reported multilayered TiC/*a*-C nanocomposite coatings consisting of well aligned and randomly oriented TiC nanocystallites that are separated by amorphous carbon sublayers.[6] The point we like to make in this paper is that these kinds of multilayers may serve as perfect interior markers for distinguishing various deformation patterns and morphologies, which can hardly be detected in a homogeneous structure.

This letter concentrates on the nanoindentation behavior and corresponding deformation mechanisms of the nanocomposite coatings under depth sensing indentation, using combined *ex situ* nanoindentation followed by cross-sectional transmission electron microscopy (XTEM). Through the examination of the displacement of TiC nanocrystallites, *a*-C sublayers and various interfaces at high resolution levels, an interparticle deformation process involving rearrangement of TiC nanocrystallites and displacement of *a*-C matrix is demonstrated that dominates the deformation mechanism at length scales ranging from tens of nanometers down to 1 nm.

The TiC/*a*-C nanocomposite coatings were deposited on ⟨100⟩ oriented Si wafer.[6] An intermediate CrTi layer was deposited between the substrate and the top coating to improve adhesion. Depth sensing indentation with a Berkovich diamond indenter was performed in a MTS Nanoindenter XP® system. XTEM observations of the nanostructure were carried out before and after indentation in a JEOL 2010F HRTEM operating at 200 kV. For postindentation XTEM investigation, a special design with an array of nanoindentations (up to 400) is used. Two indented specimens were glued face to face, followed by slicing, grinding, dimpling, and finally ion thinned to electron transparency using a Gatan PIPS operated at 3.5 kV. Compared to the focused ion beam milling method used to prepare XTEM specimen from a specific area, the present method allows intentional interruption and a restart of the ion thinning process. Therefore, extremely thin region of interesting areas can be readily obtained for atomic scale high resolution observations.

The deposition parameters and the properties of two nanocomposite coatings are listed in Table I, with the coatings named according to the atomic ratio of C and Ti. Nanoindentation derived harness H and modulus E are also listed in Table I, together with the ratios of H^3/E^2 and H/E known as the stronger indicator of resistance to plastic deformation in loaded contact and the elasticity index or "elastic strain to failure,"[7] respectively. These values suggest a reasonable deformation and wear resistance of the nanocomposite coatings. Scanning electron microscopy top views of the impressions indented into a maximum depth of 1200 nm, almost penetrating through the entire coating thickness (1.3 μm), confirm no radial cracks formed along the indenter corners but only a couple of tiny side cracks due to large tensile strain at the edges (not shown here). From the load-versus-depth curves, the coatings $C_{85}Ti_{15}$ and $C_{73}Ti_{27}$ show a residual indentation depth of 53.4% and 51.8%, respectively, of the total indentation depth.

Figure 1 shows the typical cross-sectional morphology of the indents in the coating $C_{73}Ti_{27}$. No detectable microcracks or delamination at various interfaces are observed in both the coatings, not even at such a large indentation depth. One of the common features of the indented top coatings is the permanent bending of the multilayers adapting the geometry of the indenter tip, which is accompanied geometrically by an in-plane extension. At the same time, a resultant reduction in the bilayer spacing up to ~50% was observed underneath the indent, in accordance with the residual indentation depth. Close observation reveals that, according to the deformation characteristics, the imprint can be roughly divided into five characteristic areas symmetrically located un-

[a)]Author to whom correspondence should be addressed. Tel.: +31-50-363 4898. FAX: +31-50-363 4881. Electronic mail: j.t.m.de.hosson@rug.nl.

TABLE I. Coating thickness t, multilayer periodicity Λ, TiC particle size d, and volume fraction V_F, and mechanical properties including hardness (H) and Young's modulus (E). The ratios H/E and H^3/E^2 are related to the elastic strain to failure (elasticity index) and the resistance to plastic deformation, respectively.

Coating	$t(\mu m)$	Λ (nm)	d (nm)	V_F (%)	H (GPa)	E (GPa)	H/E	H^3/E^2 (GPa)
$C_{85}Ti_{15}$	1.30	7.5	2–4	27.4	19.1	195.2	0.098	0.183
$C_{73}Ti_{27}$	1.29	11.4	4–6	52.4	21.1	207.9	0.101	0.217

derneath the indenter tip as indicated in Fig. 1. The areas A, C, and C', where the stress state is dominated by normal stress, are primarily characterized by layer densification; while the areas B, and B', where shear stress dominates, are characterized by intense shear deformation. The shear deformation of the interlayer results in two sharp wedges along the intense shear zones distributed symmetrically, but no cracking. This indicates a rather tough and adherent character of the interlayer.

The following observation and discussion will focus on the nanoscale deformation inside the nanocomposite top coating. At a moderate magnification, shear bands distributing symmetrically on both sides of the indent are revealed under proper imaging conditions (not shown). It is noteworthy that many homogeneously distributed shear bands are observed, rather than a few highly localized ones that are the common deformation mechanism in bulk amorphous materials. In addition, these shear bands are of short range characters propagating only several nanolayers rather than crossing the entire cross section of a coating.

Atomic scale high resolution XTEM reveals in detail the deformation behavior of TiC nanoparticles and the a-C tissue phase underneath the indenter. Figure 2(a) shows the original multilayered nanocomposite structure of the coating $C_{73}Ti_{27}$. It consists of alternating a-C sublayers and Ti-rich sublayers. The Ti-rich sublayers contain more than 1 ML of TiC nanocrystallites such that the TiC nanocrystallites near the Ti-on-C interface almost touch each other but those near the C-on-Ti interface are more loosely distributed in a-C phase. In correspondence with the compressed periodicity of the multilayers after indentation, the particle spacing between two adjacent Ti-rich sublayers in the area A (see Fig. 1) has been decreased noticeably [Fig. 2(b)]. That is to say, the in-plane extrusion and densification of the a-C sublayers are mainly the result of the severe indentation. In addition, the configuration of the nanoparticles in the Ti-rich sublayers also changes by means of remarkable displacement and rearrangement. Each Ti-rich sublayer after indentation is composed of a monolayer of TiC nanocrystallites well separated by the a-C tissue phase [Fig. 2(b)]. The separation is about 1–2 nm thickness, much larger than that before indentation (less than 1 nm). This kind of reconfiguration of the nanoparticles can happen only when a remarkable sliding between TiC nanocrystallites is accompanied with significantly plastic flow of the a-C matrix under the huge strain gradient inside the indent. The flow of the a-C matrix happens not only in the a-C sublayers but also in the very thin intralayer regions separating the nanoparticles in the Ti-rich sublayers,

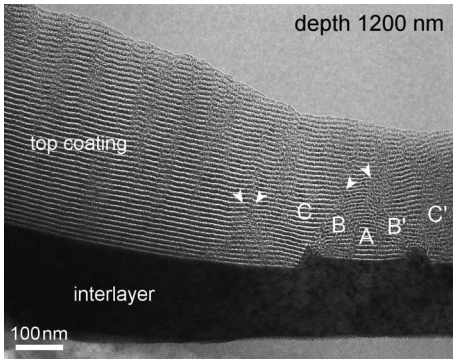

FIG. 1. Cross-sectional morphology of an indent in the coating $C_{73}Ti_{27}$, with arrows pointing to the shear bands.

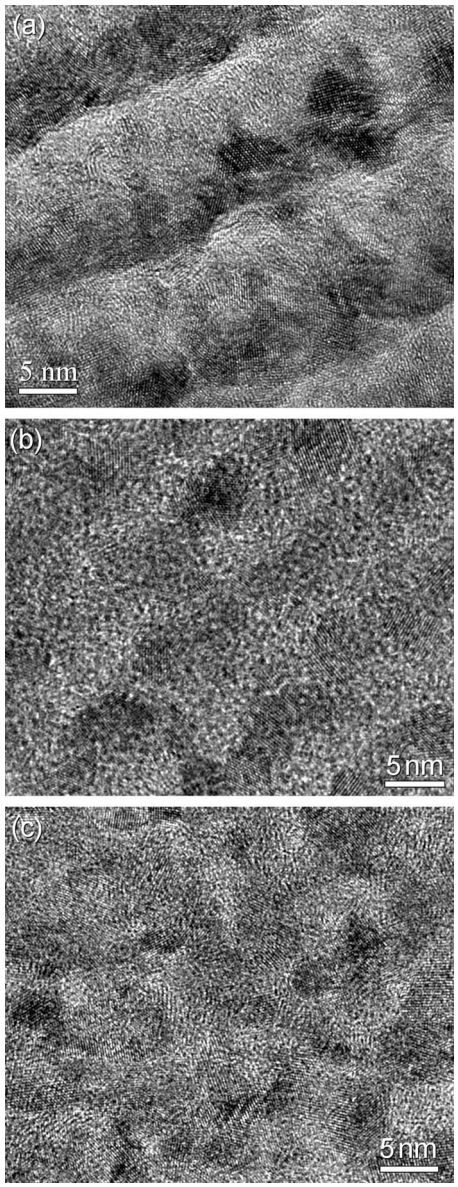

FIG. 2. High resolution XTEM micrographs showing the nanostructure before indentation (a) and after indentation in the densified area A (b) and in the intensely sheared area B (c), as indicated in Fig. 1.

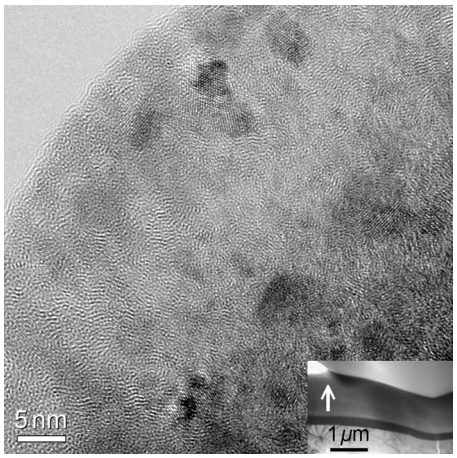

FIG. 3. XTEM micrographs showing a pileup appearing in the coating $C_{85}Ti_{15}$, indicated by an arrow in the overview of the indent, with the extrusion composed mainly of *a*-C embedded with a few TiC nanocrystallite and dense TiC nanocrystallites packed behind the extrusion (to the right-bottom corner of the micrograph).

resulting in an interparticle process of plastic deformation.

Within the regions bearing intense shear deformation (see the area *B* and *B'* in Fig. 1), well defined nanolayers become diffuse after the intensive shear strain. Under high magnification, these regions show a homogeneous structure characterized by random and uniform distribution of the nanoparticles, with the particle size unchanged [Fig. 2(c)]. This indicates a relative movement of the nanoparticles following the shear deformation and mixing of the nanoparticles from adjacent Ti-rich sublayers. The random and homogeneous distribution of TiC nanocrystallites is a result of the intersection between in-plane deformation and shear banding inclined to the sublayers as indicated in Fig. 1. Within individual TiC nanocrystallites, plastic deformation hardly occurs due to their intrinsic high strength and suppressed dislocation activity resulting from the nanometer sizes. The deformation is mainly accommodated by an interparticle-mediated process, namely, nanoparticle sliding mediated by displacement of the *a*-C matrix under the high strain gradient.

The interparticle deformation process is more pronounced in the coating $C_{85}Ti_{15}$ that contains a higher volumetric fraction of *a*-C matrix. The relative motion and changes in the *a*-C matrix and TiC nanocrystallites occur at much larger length scales (>20 nm) in comparison to the above observed rearrangement of the nanoparticles in the coating $Ti_{73}C_{27}$, attributed to the increased volumetric fraction of the moving *a*-C matrix in the coating $C_{85}Ti_{15}$. Importantly, the extensive displacement and rearrangement of TiC nanocrystallites along with the *a*-C matrix do not lead to distinguishable nanocracks or nanocavities in any way. No cracks or voids are observed in the matrix or at the interfaces of *a*-C/TiC nanocrystallites in this coating. Especially, a pileup may occur at the border of a nanoindentation as shown in the inset of Fig. 3. Under high resolution XTEM observation, the outmost part (about 50 nm thickness) of the pileup region shows a very bright contrast. The HRTEM micrograph in Fig. 3 reveals that this surface region is composed mainly of *a*-C matrix embedded with very few TiC nanocrystallites. It indicates an outflow of the *a*-C matrix to the front of the pileup. Behind this front there is a region composed of dense nanoparticles due to the outward flow of *a*-C matrix. This process is accompanied by a rearrangement of the nanoparticles and, as a result, the original multilayered structure is transformed to a homogeneous nanocomposite structure.

The shear delocalization effect is strongly evidenced by the dissipation of propagating shear bands in the indentations of large penetration depths (Fig. 1), in which abrupt shear bands arise, in fact, from the interlayer and subsequently propagate to the top layer. Examinations of several deep indentations reveal that, after crossing the interface, an abrupt shear deformation is invariably extended to a certain width (up to ~50 nm), and the shear displacement gradually fades away after propagating a small distance (not more than 150 nm), clearly demonstrating shear delocalization effect according to a decreasing shear strain.

In summary, nanoscale deformation in the multilayered TiC/*a*-C nanocomposite coatings has been revealed by combined *ex situ* nanoindentation and XTEM, with the aids of the multilayers serving as intrinsic nanomarkers to distinguish the evolution of nanostructures after indentation. The multilayered nanocomposite coatings exhibit a prominent plasticity while maintain high hardness. Interparticle processes, including rearrangement and sliding of TiC nanocrystallites with respect to the *a*-C matrix, occur in various length scales (from <10 to tens of nanometers), assisted by the flow of the *a*-C matrix. Because of the nanoscaled geometric constraint, shear deformation was brought under control by multiple shear bands, with each band contributing to plastic deformation but propagating only in nanometer scales and conveying a shear strain not large enough to cause local damage. The observed interparticle deformation mechanism facilitated by the separating *a*-C phase provides useful clues for the design of nanocomposites composed of hard nanocrystallites and a compliant matrix.

This research was carried out under the Project No. MC7.06246 in the framework of the research programme of the Netherlands Materials Innovation Institute (M2i), the former Netherlands Institute for Metals Research, Delft, the Netherlands. The authors acknowledge financial support from the M2i and the Foundation for Fundamental Research on Matter (FOM-Utrecht), the Netherlands.

[1] J. Robertson, Mater. Sci. Eng., R. **37**, 129 (2002).
[2] Y. T. Pei, D. Galvan, and J. Th. M. De Hosson, Acta Mater. **53**, 4505 (2005).
[3] M. G. Fyta, I. N. Remediakis, P. C. Kelires, and D. A. Papaconstantopoulos, Phys. Rev. Lett. **96**, 185503 (2006).
[4] S. Namilae, B. Radhakrishnan, and G. B. Sarma, Compos. Sci. Technol. **67**, 1302 (2007).
[5] I. N. Remediakis, M. G. Fyta, C. Mathioudakis, G. Kopidakis, and P. C. Kelires, Diamond Relat. Mater. **16**, 1835 (2007).
[6] Y. T. Pei, C. Q. Chen, K. P. Shaha, J. Th. M. De Hosson, J. W. Bradley, S. A. Voronin, and M. Čada, Acta Mater. **56**, 696 (2008).
[7] Y. T. Pei, P. Huizenga, D. Galvan, and J. Th. M. De Hosson, J. Appl. Phys. **100**, 114309 (2006).